

This document is downloaded from DR-NTU, Nanyang Technological University Library, Singapore.

Title	High frame rate photoacoustic imaging using clinical ultrasound system
Author(s)	Sivasubramanian, Kathyayini; Pramanik, Manojit
Citation	Sivasubramanian, K., & Pramanik, M. (2016). High frame rate photoacoustic imaging using clinical ultrasound system. Proceedings of SPIE 9708, Photons Plus Ultrasound: Imaging and Sensing 2016, 9708, 97084Q-6.
Date	2016
URL	<a href="http://hdl.handle.net/10220/41441">http://hdl.handle.net/10220/41441</a>
Rights	© 2016 Society of Photo-optical Instrumentation Engineers (SPIE). This paper was published in Proceedings of SPIE 9708, Photons Plus Ultrasound: Imaging and Sensing 2016 and is made available as an electronic reprint (preprint) with permission of SPIE. The published version is available at: [ <a href="http://dx.doi.org/10.1117/12.2209037">http://dx.doi.org/10.1117/12.2209037</a> ]. One print or electronic copy may be made for personal use only. Systematic or multiple reproduction, distribution to multiple locations via electronic or other means, duplication of any material in this paper for a fee or for commercial purposes, or modification of the content of the paper is prohibited and is subject to penalties under law.

# High frame rate photoacoustic imaging using clinical ultrasound system

Kathyayini Sivasubramanian, and Manojit Pramanik\*

School of Chemical and Biomedical Engineering, Nanyang Technological University, Singapore 637459

## ABSTRACT

Photoacoustic tomography (PAT) is a potential hybrid imaging modality which is gaining attention in the field of medical imaging. Typically a Q-switched Nd:YAG laser is used to excite the tissue and generate photoacoustic signals. But, they are not suitable for clinical applications owing to their high cost, large size. Also, their low pulse repetition rate (PRR) of few tens of hertz prevents them from being used in real-time PAT. So, there is a growing need for an imaging system capable of real-time imaging for various clinical applications. In this work, we are using a nanosecond pulsed laser diode as an excitation source and a clinical ultrasound imaging system to obtain the photoacoustic imaging. The excitation laser is  $\sim 803$  nm in wavelength with energy of  $\sim 1.4$  mJ per pulse. So far, the reported frame rate for photoacoustic imaging is only a few hundred Hertz. We have demonstrated up to 7000 frames per second framerate in photoacoustic imaging (B-mode) and measured the flow rate of fast moving object. Phantom experiments were performed to test the fast imaging capability and measure the flow rate of ink solution inside a tube. This fast photoacoustic imaging can be used for various clinical applications including cardiac related problems, where the blood flow rate is quite high, or other dynamic studies.

**Keyword:** Photoacoustic tomography, Hybrid imaging, High frame rate, Pulsed laser diode.

## 1. INTRODUCTION

Photoacoustic tomography (PAT) is an imaging technique which is rapidly gaining importance in the field of biomedical imaging. It is a hybrid, noninvasive imaging modality which combines the high contrast of optical and the high resolution of ultrasound imaging.<sup>1-4</sup> Non-ionising laser pulses are used to irradiate the sample (e.g., biological tissues), which leads to the absorption of light energy to increase the local temperature (in the order of a few milli degrees) which results in thermoelastic expansion and further to the release of pressure waves known as photoacoustic (PA) waves. Ultrasound detectors (single or multiple or array detectors) are used to acquire the PA waves outside the sample. PAT has several advantages in comparison to other optical imaging techniques like optical coherence tomography including deeper penetration depth, good spatial resolution, and high soft tissue contrast. Ultrasound scattering is two to three orders of magnitude less than the optical scattering in biological tissues, which makes photoacoustic imaging overcome the fundamental depth limitations of already existing pure optical imaging. It has a range of potential clinical applications, including breast cancer imaging, brain imaging, sentinel lymph node imaging, temperature monitoring, and many others.<sup>5-10</sup> PAT imaging requires contrast agents. Blood, melanin etc., act as intrinsic contrast agents. When the signal is not strong enough from these, other exogenous contrast agents can be used like the gold nanoparticles, nanospheres, carbon nanotubes etc.<sup>11-14</sup>

Biological tissues have higher penetration of light in the Near-infrared (NIR) region. High frame rate PA imaging is needed in applications where imaging of a small region, undergoing rapid changes, needs to be performed in real time and very fast. Few possible applications where high frame rate PAT system could be used are imaging of the movement of the heart valves, shape of heart, myocardial functions, or even monitoring circulating tumor cells in blood vessels. The velocity of the blood in the aorta is 40 cm/s, in vena cava is 15 cm/s, and in the capillaries is 0.03 cm/s.<sup>15</sup> Another area where this can prove useful is in the real time imaging of the circulating tumor cells (CTC) in the blood stream, which acts as an indicator for metastasis of cancer. Particularly for melanoma cells as it has a very strong light absorption in the NIR wavelengths even against blood contrast. Another potential area of application is to image the

\* Email: manojit@ntu.edu.sg

heartbeat of rodents; they have approximately 400 beats per minute which can be imaged using the high speed PAT system.<sup>16</sup>

Usually a Nd-YAG laser is used as source of light in the NIR region which can pump the light using the OPO laser or a dye laser. The major disadvantage with this system is that the pulse repetition frequency (10-20 Hz) is low, very bulky, not portable and hence, not suitable for clinical translation of the PAT system. Pulse laser diode (PLD) on the other hand has a high pulse repetition frequency, very compact, portable and can be translated into the clinical setup very easily.<sup>17, 18</sup> So far, literature shows PAT imaging with only a few tens of frames per second (fps). There are two different types of PAT systems. The first type uses a single element ultrasound transducer. Recently, it was shown that low cost, portable PAT systems can be built with reasonable imaging depth (up to 2 cm) with a single element transducer.<sup>19</sup> So far, this is the fastest reported PAT system with single element transducer with a cross-sectional PAT imaging speed of 3 sec. Most conventional PAT systems with single element transducer will take up to several minutes to take one cross-sectional PAT image. The second type of PAT system uses ultrasound array transducer and a parallel data acquisition system. The clinical ultrasound imaging system can be incorporated for photoacoustic imaging and modified to obtain better results.<sup>17, 18, 20, 21</sup> A clinical ultrasound imaging system allows the user to choose the type of array transducers (linear, convex, phased array etc.) depending on the application areas giving more flexibility. With the clinical ultrasound imaging systems real time phantom imaging was done at 20 fps up to 15 mm depth.<sup>17</sup> In another study performed with an OPO-Ultrasound system, *in vivo* real time imaging of blood vessels in rat was done at 20 fps.<sup>20</sup> Thus, the maximum frame rate reported till now for photoacoustic tomography is 20 fps.

In this work, we use a low cost, portable pulsed laser diode (PLD) to demonstrate up to 7000 fps PAT imaging (B-scans). The maximum pulse repetition frequency of the PLD is 7000 Hz with a maximum pulse energy of ~1.4 mJ. The combination of the PLD and clinical ultrasound imaging system made very high frame rate photoacoustic B-scan imaging possible. Phantom experiments were performed to demonstrate the high frame rate imaging. To demonstrate the high frame rate PAT imaging, black ink flowing inside a tube was used at various flow rates from 3 cm/s to 14 cm/s. From the PA images we were able to measure the flow rate accurately as well. For comparison, a low pulse repetition rate Nd:YAG pumped OPO laser (standard laser used for most PAT system) based PA imaging, as well as normal ultrasound imaging were also done.

## 2. MATERIALS AND METHODS

The experimental set up is shown in Fig. 1 (a). A clinical research ultrasound system (ECUBE 12R, Alpinion, South Korea) capable of imaging both photoacoustic imaging as well as ultrasound imaging was used. For the system to be operated in the photoacoustic mode, laser excitation is provided. The controlling unit synchronizes the laser excitation and ultrasound detection. In order to perform high frame rate PAT imaging the pulsed laser diode (Quantel DQ-Q1910-SA-TEC) provides ~136 ns pulses at a NIR wavelength of 803 nm, and maximum pulse energy of ~1.4 mJ. It has a maximum pulse repetition frequency of 7000 Hz. The PLD generates a diverging laser beam rectangular in shape. The PLD is controlled by the laser driver unit (LDU) which consists of a temperature controller (LaridTech, MTTC1410), a 12 V power supply (Votcraft, PPS-11810), a variable power supply (to vary the laser output power), and a function generator (to control the laser repetition rate). The pulse energy and repetition rate can be controlled individually with variable power supply (BASETech, BT-153), and function generator (FG250D, Funktionsgenerator), respectively. The function generator provides a TTL (Transistor-Transistor Logic) signal which synchronizes the laser excitation and the ultrasound data acquisition by the clinical ultrasound system. A cylindrical lens (CL) was used in front of the laser window in order to make the laser beam narrower. The laser beam spot was around 15 mm x 5 mm on the sample. The generated photoacoustic signals were acquired by a linear array transducer (L3-12 transducer, compatible with the Ecube ultrasound system) consisting of 128 array elements. This setup is call as PLD-PAT system. A similar set up was done with the OPO laser, due to its low pulse repetition rate, this sytem cannot provide real-time PAT imaging. The excitation source, consists of the OPO (Continuum, Surelite OPO) laser pumped by a 532 nm Nd:YAG pump laser (Continuum, Surelite Ex). The OPO generates 5 ns duration pulses at 10 Hz repetition rate with wavelength tunable from 680 nm to 2500 nm. For the experiments it was tuned to 803 nm since the PLD also operates at that wavelength. The beam spot size of the laser falling on the sample is ~1.5 cm in diameter. The PA images were captured by the L3-12 linear array transducer in the Ecube ultrasound imaging system. To synchronize the data acquisition the trigger out from the pump laser is connected to the Ecube system. This setup is called as OPO-PAT system.

For PAT imaging the Ecube ultrasound system needs to be operated in the research mode. In this mode, the instructions are coded using a python script to assign the various parameters. The PA signal is acquired by the array transducer L3-12, which has 128 array elements which has an active area is 3.85 cm x 1 cm. Fig. 1(b) shows the

functioning of data acquisition in photoacoustic mode. The data acquisition is done by 64 channels of the receiver each time. This is fixed and cannot be modified. The system can be operated in two different modes. In mode one, there are two frames per PA image (requires two trigger from the laser), thus the effective frame rate is half the laser repetition rate. In this mode, we could achieve a maximum frame rate of 3500 fps using PLD and 5 fps using the OPO laser. On the other hand in mode two, only 64 elements can be used and requires only a single laser pulse trigger to capture a B-mode PA image. Thus, the frame rate of the PA images is same as the laser pulse repetition rate. In this mode, we could achieve a maximum frame rate of 7000 fps using PLD and 10 fps using the OPO laser. The results shown here are with the PA system being operated in mode two, i.e., 7000 fps with PLD and 10 fps with OPO laser excitation. The acquired PA signals then go through a series of inbuilt filters for the image processing and the output PA image is seen on the monitor. At the same time raw channel data, beam formed and scan converted data can also be saved on the hard drive of the Ecube system. These saved frames were later processed in MATLAB for measuring the flow rate as well as to create the movie clips.

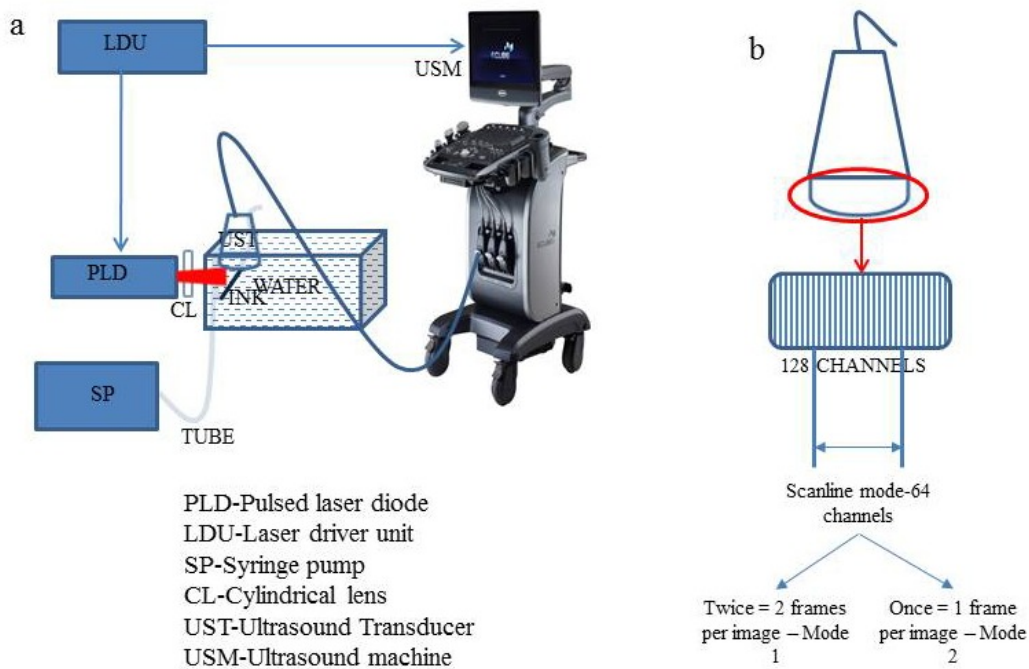


Fig. 1. a) Schematic of the PLD-PAT ultrasound setup; b) The L3-12 linear array ultrasound transducer which can be operated in 2 different modes. Mode 1- using all the 128 arrays elements; Mode 2- using 64 elements only (element numbers 1-64 or 65-128).

For comparison B-mode ultrasound imaging was also performed in the ultrasound mode. For this the system operates internally and no external trigger is needed. The L3-12 ultrasound transducer performed both sending and the receiving of ultrasound waves. The system can save all types of ultrasound data (RF signals, IQ data, Beam formed data, and Scan converted data) for post processing. However, no post processing was done for the ultrasound images.

To demonstrate the high frame rate PA imaging, flow imaging was done. A low density polyethylene (LDPE) transparent tube of inner diameter 1.15 mm was placed in the water bath on which focussed the laser beam falls. Black ink (which has strong optical absorption at 803 nm wavelength) was injected into the tube using a 10 mL syringe with a 24G needle. The flow rate of black ink was controlled with a programmable syringe pump (AL-1000, World precision instruments). The transducer was placed at a distance of 1 cm from the tube with a total imaging depth of 2 to 3 cm. The various flow rates that were used for the experiments are 3 cm/s, 6 cm/s, 10 cm/s, and 14 cm/s. The flow rates were chosen in order to demonstrate the high frame rate PA imaging system imaging and accurately finding the different flow rates from the PA images is feasible. The flow rate of the ink can be calculated from the PA images. The ultrasound transducer has 128 array elements with elements size of 0.03 cm. Based on the beam forming parameters, on the PA

image there are 128 pixels along the x-axis (each pixel size is 0.03 cm). From the saved PA image the distance moved by the ink in a given period of time was calculated. A start frame and an end frame was chosen, if the ink flow has moved by a distance  $d$  in  $N$  frames ( $N = \text{end frame number} - \text{start frame number}$ ), then  $\text{Flow rate } (F) = d/N$ .

### 3. RESULTS AND DISCUSSIONS

It is shown here that with B-mode ultrasound imaging it is not possible to see the ink flow, as it does not possess any ultrasound contrast. However, ink being a good optical contrast agent, will be visible in photoacoustic imaging. Fig. 2 shows the screenshot of the ultrasound B-mode image obtained with the Ecube. A depth of 2 cm was imaged when the transducer was placed at a distance of 1 cm from the tube with ink flow. The flow rate of the black ink was maintained at 6 cm/s. The tube part of the image alone is enlarged and shown on the right. In the ultrasound image only the LDPE tube boundaries are visible. The flow of the ink is not visualized as it is not a good ultrasound contrast.

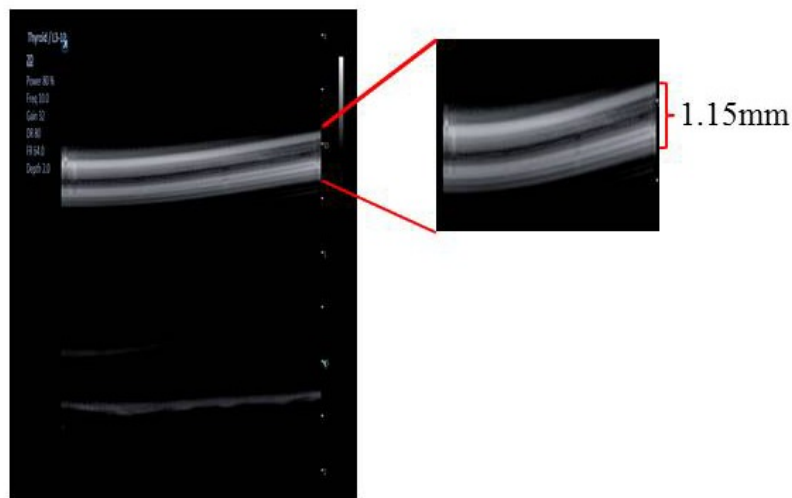


Fig. 2: Ultrasound B-mode image showing the flow of the black ink inside the tube. The enlarged tube region shows that the boundary of the tube can be seen clearly, but not the ink flow in the ultrasound images, as it does not have a good ultrasound contrast.

PA imaging was done at different flowrates. Fig. 3 shows the PA B-scan images obtained from the PLD-PAT system. Shown is the flow of the ink in the tube at various given time points. 7000 fps PA B-scan images were recorded. The PA images represented here are at time points  $t = 0$  s [Fig. 3(a)], 0.05 s [Fig. 3(b)], 0.1 s [Fig. 3(c)], and 0.25 s [Fig. 3(d)]. For representative purpose only velocity of 6 cm/s is shown here. The flow of the ink moving inside of the tube can be clearly observed from the figures. The set of images here shows the flow of the ink for a time period of 0.25 s. The gradual flow of the ink can be observed at different time points, as observed from the images. The beam width of the laser is 15 mm which is almost consistent the distance moved by the ink.

The same sets of experiments were carried out with OPO-PAT system. PA images were recorded at 10 fps. However, the gradual flow of the ink in the tube could not be observed. We have not included the images for the same. The ink flow happened within one frame only for the entire 15 mm beam width. Due to the low pulse repetition rate of 10 Hz of the OPO laser the flow can't be visualized as done with PLD-PAT system.

To validate that the high frame rate imaging is accurate, the flowrate from the images were calculated as described earlier. The flowrate as noted from the syringe pump is 6 cm/s and the calculation from the image was 6.5 cm/s, which is consistent with the input flow rate. The maximum possible framerate with the current PLD-PAT system is 7000 fps. This is limited by the excitation laser source pulse repetition rate, data acquisition modes, imaging depth etc. Up to 14 cm/s ink flow rate PA imaging was demonstrated in this work. However, much higher flowrates can be visualized with the system. The distance of each pixel on the PA image is 0.3 mm. Hence, the theoretical maximum flowrate that can be captured by this system is 134.4 m/s.

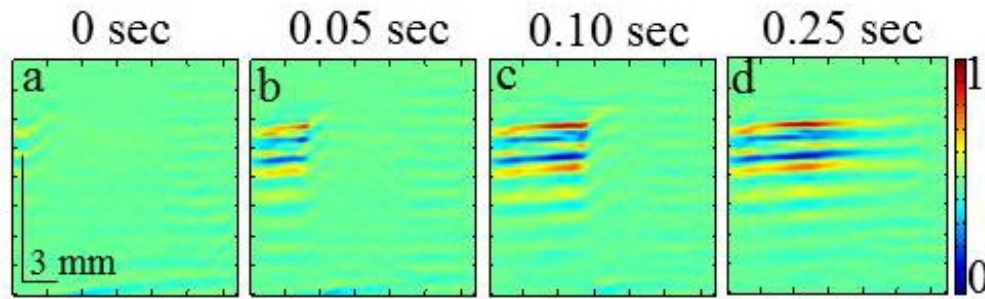


Fig. 3. Set of PA images showing the flow of ink at different time points obtained with PLD-PAT system. Imaging was done at 7000 fps frame rate. Flowrate is 6 cm/s. All images have same scale bars shown in (a). The normalised colormap is shown on the right.

**Laser safety:** When PAT is used to image subjects *in vivo*, the maximum permissible pulse energy and the maximum permissible pulse repetition rate are governed by the ANSI laser safety standards.<sup>22</sup> The safety limits for the skin depend on the optical wavelength, pulse duration, exposure duration, and exposure aperture. In the spectral region of 700-1050 nm, the maximum permissible exposure (MPE) on the skin surface by any single laser pulse should not exceed  $20 \times 10^{2(\lambda-700)/1000} \text{ mJ/cm}^2$  ( $\lambda$  is the wavelength in nm).<sup>22</sup> Therefore, at 803 nm the MPE is  $\sim 31 \text{ mJ/cm}^2$ . The MPE for exposure time  $t = 2 \text{ sec}$  is  $1.1 \times 10^{2(\lambda-700)/1000} \times t^{0.25} \text{ J/cm}^2$  ( $= 1.1 \times 10^{2(803-700)/1000} \times 2^{0.25} \text{ J/cm}^2 = 2.07 \text{ J/cm}^2$ ). Since the PLD is operating at 7000 Hz (total number of laser pulses =  $2 \times 7000 = 14000$ ), the MPE becomes  $0.15 \text{ mJ/cm}^2$  ( $2.07/14000$ ) per pulse. In this imaging system, the pulsed diode laser provides maximum  $\sim 1.4 \text{ mJ}$  pulse energy and the laser beam spread over an area  $\sim 0.75 \text{ cm}^2$  ( $\sim 1.5 \text{ cm} \times 0.5 \text{ cm}$ ). Therefore, the laser fluence is  $\sim 1.9 \text{ mJ/cm}^2$ . Therefore, at present in the PLD-PAT, the fluence is above the MPE.

For OPO excitation, the OPO laser energy output was at  $\sim 40 \text{ mJ}$  per pulse at 803 nm on the sample surface ( $\sim 1.5 \text{ cm}$  diameter spot). Thus the fluence on the sample surface was  $\sim 22.6 \text{ mJ/cm}^2$ . Thus the fluence is well within the ANSI safety limit. In this work, as only phantoms were imaged, the MPE safety limit was not strictly adhered to in case of PLD-PAT system. Moreover, the aim was to show that high frame rate imaging is possible and hence, no frame averaging was done to improve the signal-to-noise ratio. For future *in vivo* experiments, the fluence can be reduced by spreading the beam over a larger area or reducing the pulse repetition rate or reducing the laser power output by controlling the power supply itself or reducing the exposure time also.

#### 4. CONCLUSION

We have shown that high frame rate photoacoustic imaging of 7000 fps is possible using the PLD-PAT clinical ultrasound system. On the other hand, with the OPO laser only 10 fps (max) PA imaging is possible. With the high frame rate of 7000 fps flow rate up to 134.4 m/s (theoretical) can be captured. It was shown that the flow can be visualized and also accurate flow measurements can be done from the PA B-mode images obtained from the PLD-PAT system with various flow rates. Further studies will be conducted to explore the various *in vivo* applications in future, where high frame rate PA imaging would be beneficial like imaging circulating tumor cells, heart valves, blood vessel etc. The PLD being low cost, portable, and easy to handle may be easier to translate to clinical applications.

#### ACKNOWLEDGEMENTS

The authors would like to acknowledge the financial support from the Tier 1 grant funded by the Ministry of Education in Singapore (RG31/14: M4011276).

#### REFERENCES

- [1] Taruttis, A., and Ntziachristos, V., "Advances in real-time multispectral optoacoustic imaging and its applications," *Nature Photonics*, 9(4), 219-227 (2015).

- [2] Wang, L. V., and Hu, S., "Photoacoustic Tomography: In Vivo Imaging from Organelles to Organs," *Science*, 335(6075), 1458-1462 (2012).
- [3] Wang, L. V., "Prospects of photoacoustic tomography," *Medical Physics*, 35(12), 5758-67 (2008).
- [4] Wang, L. V., "Multiscale photoacoustic microscopy and computed tomography," *Nature Photonics*, 3(9), 503-509 (2009).
- [5] Li, R., Wang, P., Lan, L. *et al.*, "Assessing breast tumor margin by multispectral photoacoustic tomography," *Biomedical Optics Express*, 6(4), 1273 (2015).
- [6] Diot, G., Dima, A., and Ntziachristos, V., "Multispectral opto-acoustic tomography of exercised muscle oxygenation," *Optics Letters*, 40(7), 1496-1499 (2015).
- [7] Chen, B. Z., Yang, J. G., Wu, D. *et al.*, "Photoacoustic imaging of cerebral hypoperfusion during acupuncture," *Biomedical Optics Express*, 6(9), 3225-3234 (2015).
- [8] Li, X., Heldermon, C. D., Yao, L. *et al.*, "High resolution functional photoacoustic tomography of breast cancer," *Medical Physics*, 42(9), 5321-5328 (2015).
- [9] Erpelding, T. N., Kim, C., Pramanik, M. *et al.*, "Sentinel Lymph Nodes in the Rat : Noninvasive Photoacoustic and US imaging with a clinical US system," *Radiology*, 256(1), 102-110 (2010).
- [10] Pramanik, M., and Wang, L. V., "Thermoacoustic and photoacoustic sensing of temperature," *Journal of Biomedical Optics*, 14(5), 054024 (2009).
- [11] Li, W., and Chen, X., "Gold nanoparticles for photoacoustic imaging," *Nanomedicine*, 10(2), 299-320 (2015).
- [12] Pramanik, M., Swierczewska, M., Green, D. *et al.*, "Single-walled carbon nanotubes as a multimodal-thermoacoustic and photoacoustic-contrast agent," *Journal of Biomedical Optics*, 14(3), 034018 (2009).
- [13] De la Zerda, A., Zavaleta, C., Keren, S. *et al.*, "Carbon nanotubes as photoacoustic molecular imaging agents in living mice," *Nature Nanotechnology*, 3, 557-62 (2008).
- [14] Yang, X., Skrabalak, S. E., Li, Z.-Y. *et al.*, "Photoacoustic Tomography of a Rat Cerebral Cortex in vivo with Au Nanocages as an Optical Contrast Agent," *Nano Letters*, 7, 3798-3802 (2007).
- [15] Gerard J. Tortora , B. D., [Principles of anatomy and physiology] John Wiley & Sons, Inc.
- [16] Toni Azar, J. S., and David Lawson, "Heart Rates of Male and Female Sprague-Dawley and Spontaneously Hypertensive Rats Housed Singly or in Groups," *J Am Assoc Lab Anim Sci*, 50(2), 175-184 (2011).
- [17] Daoudi, K., van den Berg, P. J., Rabot, O. *et al.*, "Handheld probe integrating laser diode and ultrasound transducer array for ultrasound/photoacoustic dual modality imaging," *Optics Express*, 22(21), 26365 (2014).
- [18] Daoudi, K., van den Berg, P. J., Rabot, O. *et al.*, "Handheld probe for portable high frame photoacoustic/ultrasound imaging system." 8581, 85812I.
- [19] Upputuri, P. K., and Pramanik, M., "Performance characterization of low-cost, high-speed, portable pulsed laser diode photoacoustic tomography (PLD-PAT) system," *Biomedical Optics Express*, 6(10), 4118-29 (2015).
- [20] Montilla, L. G., Olafsson, R., Bauer, D. R. *et al.*, "Real-time photoacoustic and ultrasound imaging: a simple solution for clinical ultrasound systems with linear arrays," *Physics in Medicine and Biology*, 58(1), N1-12 (2013).
- [21] Kim, C., Erpelding, T. N., Maslov, K. *et al.*, "Handheld array-based photoacoustic probe for guiding needle biopsy of sentinel lymph nodes," *Journal of Biomedical Optics*, 15(4), 046010 (2010).
- [22] Thomas, T. S., Dale, P. S., Weight, R. M. *et al.*, "Photoacoustic detection of breast cancer cells in human blood." 6856, 685609.